ICES Journal of Marine Science, 59: 140–149. 2002
doi:10.1006/jmsc.2001.1138, available online at http://www.idealibrary.com on IDEAL®

A method for estimating the "position accuracy" of acoustic fish tags

John E. Ehrenberg and Tracey W. Steig

Ehrenberg, J. E., and Steig, T. W. 2002. A method for estimating the "position accuracy" of acoustic fish tags. – ICES Journal of Marine Science, 59: 140–149.

Acoustic tag systems have been used for many years to study the behavior of fish in specific areas of interest. In particular tag systems are being used successfully to study the behavior of downstream migrating salmon smolts (*Oncorhynchus* spp.) as they approach hydro-electric dams. While field studies have demonstrated the potential for acoustic tag systems, little has been done to quantify their performance. This paper develops a method for predicting the accuracy of the "position estimates" provided by acoustic tag systems. General expressions are developed that can be applied to any particular deployment of a tag system which lead onto a method for the direct calculation of the "position error" as a function of hydrophone geometry, standard deviation of the signal arrival times, and the inaccuracies in the assumed sound velocities. This method is independent of the algorithm used to determine the position solution. Using the methods of analysis developed here some specific examples are presented that provide general guidelines that should be followed to achieve good performance when deploying an acoustic tag system.

Keywords: acoustic tags, fish movement, fish tracking, position accuracy.

Received 24 May 2000; accepted 14 September 2001.

J. E. Ehrenberg and T. W. Steig: Hydroacoustic Technology Inc., 715 NE Northlake Way, Seattle, WA 98105, USA; tel: (206) 633-3383, fax: (206) 633-5912, e-mail: Consulting@HTIsonar.com

Introduction

Acoustic tags have been used to monitor fish movement for many years. One of the earliest attempts to use acoustic telemetry was performed in 1956 by the National Marine Fisheries Service on adult chinook (*Oncorhynchus tshawytscha*) and coho salmon (*Oncorhynchus kisutch*) (Trefethen, 1956). This work was followed in 1957 by studies on the Columbia River above Bonneville Dam observing the upstream migration of Pacific salmon [chinook, coho, and steelhead (*Oncorhynchus mykis*)] in the forebay of the dam (Johnson, 1960). Subsequent acoustic telemetry studies followed and are summarized by Ireland and Kanwisher (1978), Mitson (1978), and Stasko and Pincock (1977). Although most acoustic telemetry studies with Pacific salmon have monitored adults, several studies have been performed with juvenile Atlantic salmon smolts (*Salmo salar*) as they migrate through lochs, rivers and estuaries in the United Kingdom (Thorpe *et al*., 1981; Potter, 1988; Solomon and Potter, 1988; Moore *et al*., 1990; Potter *et al*., 1992; Moore, 1995; Lacroix and McCurdy, 1996; Russell *et al*., 1998; Smith *et al*., 1998; Voegeli *et al*., 1998; O'Dor *et al*., 1998).

A sophisticated tracking system was installed in a loch in Scotland (Hawkins *et al*., 1974). Five omnidirectional hydrophones were positioned in a small loch. The fish's location was recorded every 15 minutes in order to monitor the movement of fish during night and day. It was concluded that if the system could be automated, a record could be made every second and the swimming path of each fish could then be determined.

In more recent years acoustic tags have proven to be a very valuable tool for studying salmonid smolt behavior on the Columbia and Snake rivers. Unlike other techniques such as radio tags or active acoustic systems (i.e. systems that process echoes from acoustically illuminated fish), acoustic tags provide a means of tracking a fish everywhere in the region of interest. Radio-tagged fish are primarily detected within 10 m of the surface and active acoustic systems only provide information of fish location while the fish is within the acoustic beam.

A tracking system has been developed and used for the past three years at Rocky Reach Dam on the

1054–3139/02/020140+10 $35.00/0

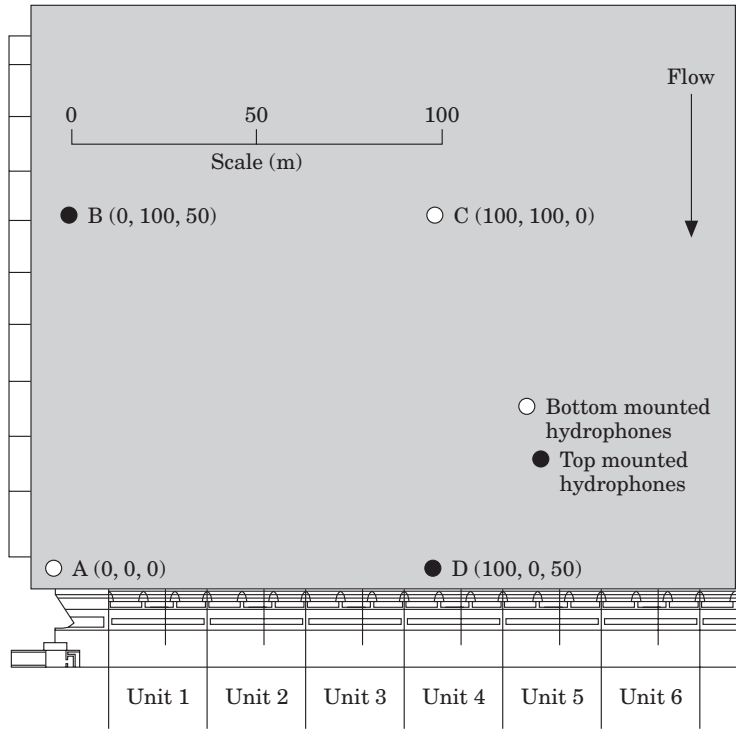

Figure 1. Plan view of a typical dam showing the four hydrophones locations.

Columbia River (Steig *et al*., 1999; Steig, 2000; Steig and Timko, 2000; Steig *et al*., 2001). Other similar studies have been conducted at Lower Granite Dam on the Snake River (Steig and Timko, 2001), Bonneville Dam on the Columbia River, Cowlitz Falls Dam on the Cowlitz River, and Chittendon Locks on the Washington Ship Canal. These studies utilized up to 32 omni-directional hydrophones placed in known locations. The acoustic tag system determines the location of the tag using the relative arrival time of the acoustic signal at a minimum of four hydrophones. Studies have been conducted to compare the theoretical with the field measured position at a Loch in Scotland (Smith *et al*., 1998). The accuracy of the position measurements provided by an acoustic tag system depend on a number of factors (Kell *et al*., 1994). The primary factors affecting accuracy include: the position of the tag relative to the location of the hydrophones, the noise level relative to the tag-signal level at the hydrophones and the accuracy of the assumed velocity of sound in the water. This paper develops a direct method for calculating the "position accuracy" of the location of acoustic tags without the need for field measurements or Monte Carlo simulations. The methods presented here can be used to select the optimum hydrophone location to provide minimum position errors prior to the actual deployment of the acoustic tag measurement system.

The principle used for determining the position of acoustic tag systems is the same as that used to determine position via the Global Positioning System, (GPS, Parkinson and Spilker, 1996). Various algorithms that have been developed for solving for GPS position and these algorithms can be used, with modifications, to estimate the position of an acoustic tag from the relative arrival times of the tag signal at a set of hydrophones. The basic approach used in these algorithms is to write

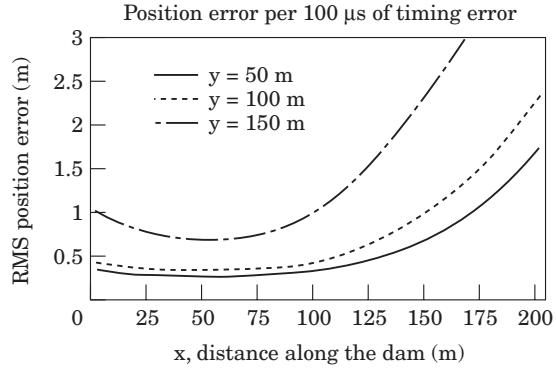

Figure 2. The effect of tag location on the accuracy of the location estimate for a mid-water depth.

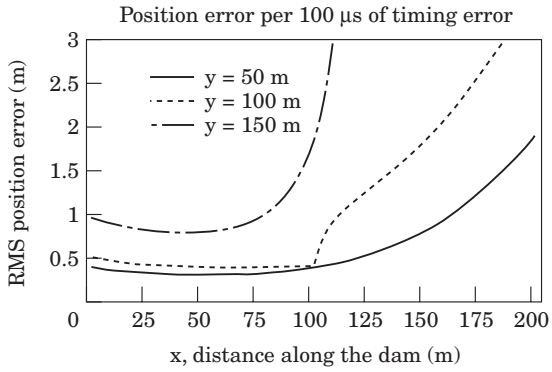

Figure 3. The effect of tag location on the accuracy of the location estimate for tag near the bottom, z=1 m.

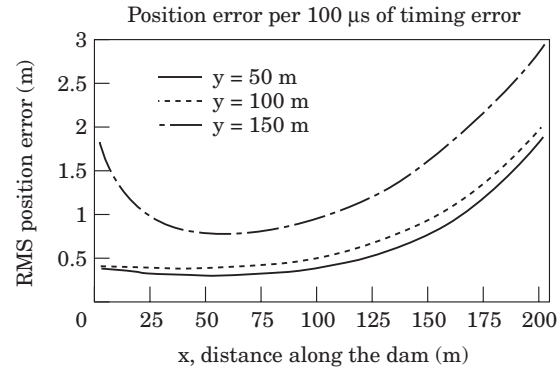

Figure 4. The effect of tag location on the accuracy of the location estimate for tag near the surface, z=49 m.

an expression for the time that it takes for the acoustic signal to travel from an assumed x, y, z location for the tag to each of the four hydrophones. Expressions can then be written for the differences in the arrival times for the signal at each of the four hydrophones. This provides a set of three time-difference equations with three unknown variables, the x, y, z locations of the tag. The x, y, z location of the tag is then determined such that the mean squared difference between the measured and calculated time differences are minimized. The position accuracy analysis does not depend on the particular method used to solve the equations.

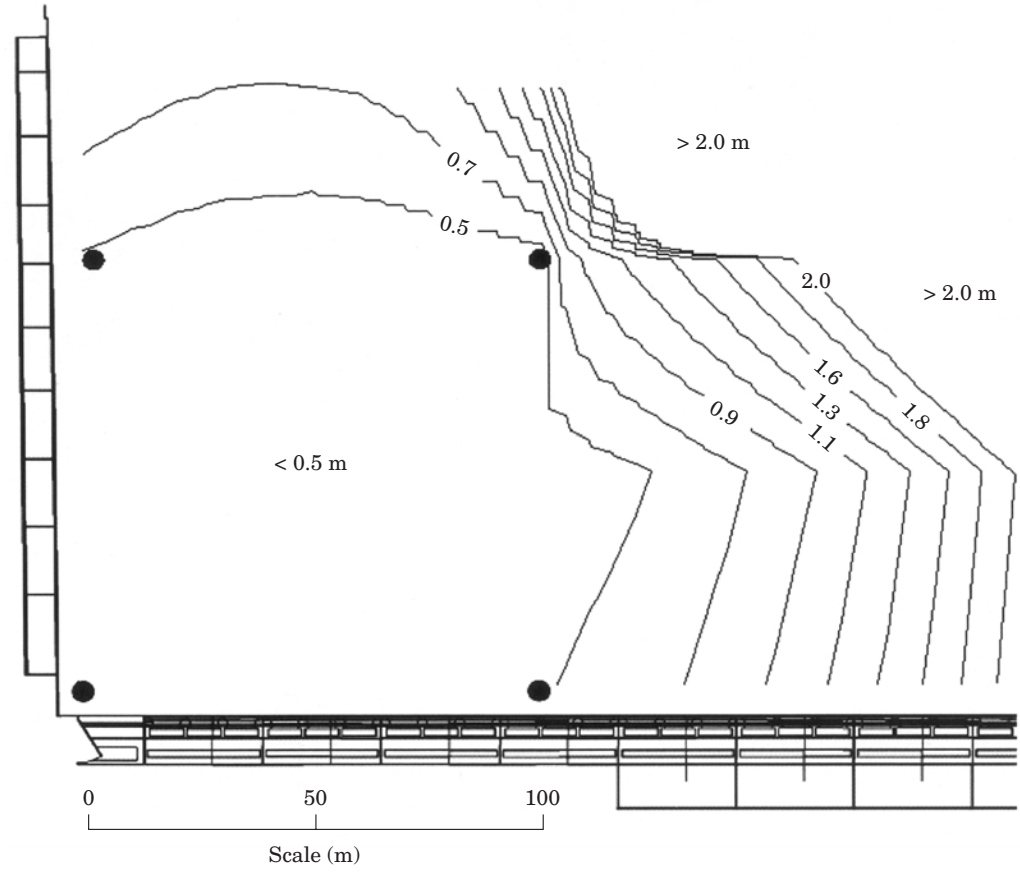

Figure 5. Plan view of the dam and hydrophone locations showing a contour plot of position errors (in m) for a depth of z=1 m.

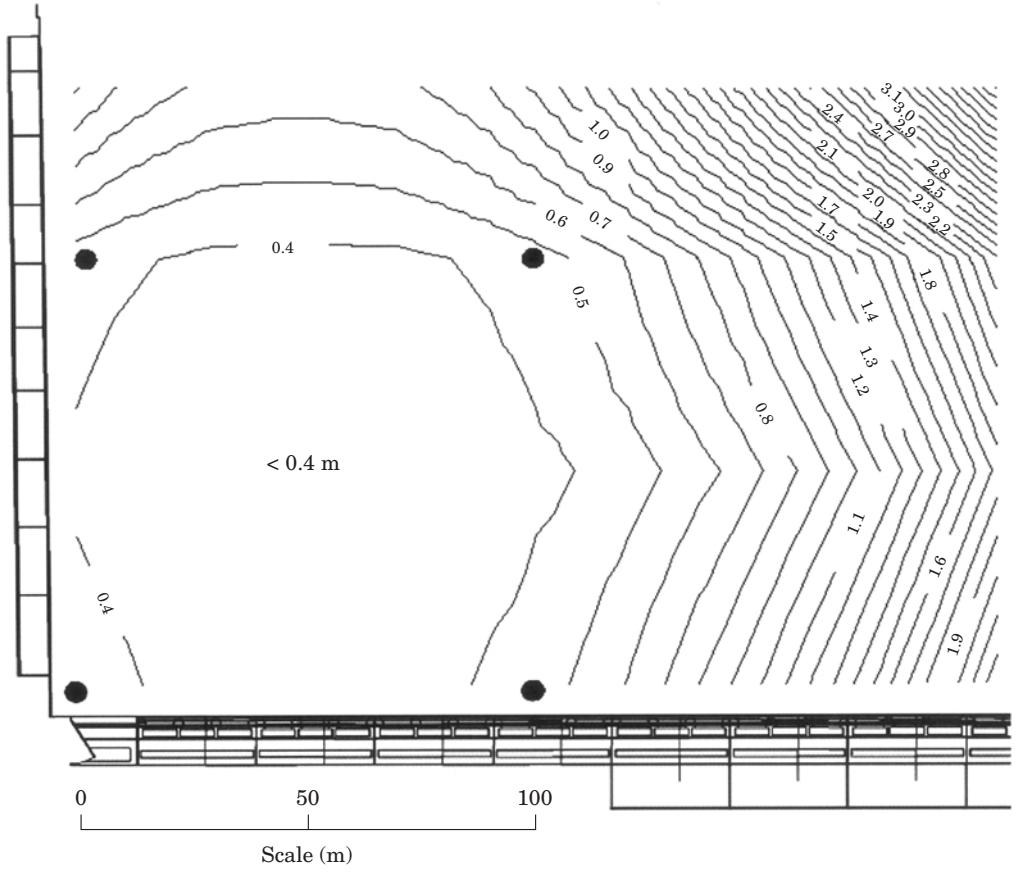

Figure 6. Plan view of the dam and hydrophone locations showing a contour plot of position errors for a depth of z=25 m.

Tag "position error" analysis

The accuracy of the tag position estimate depends on the relative location of the hydrophones and the tag. Depending on the geometry errors in the measured arrival times can affect the accuracy of the "position estimate" for the tag. The two primary sources of measured arrival-time error are the presence of noise in the received signal and errors in the accuracy of the assumed acoustic sound velocity. Appendix A contains derivations of expressions that use linear algebra and partial derivatives for the position errors resulting from arrival time variability and errors in the assumed sound velocity. In most cases the arrival-time and velocity errors cannot be directly measured. However the size of these errors can be estimated based on other parameters. In particular one of the primary sources of the arrival-time error is the presence of noise in the processed signal. Helstrom (1960) has derived an expression for the arrival-time error as a function of the signal-to-noise ratio. This can be accurately measured and therefore the arrival-time error can be predicted. Similarly the sound-velocity errors are directly dependent on inaccurate knowledge of the water temperature (Clay and Medwin, 1977). Appendix B discusses the effect of both additive noise and "quantization" error on the measured arrival-time accuracy and also derives an expression for the sound-velocity error in terms of temperature.

Application of performance analysis

A typical application for a tag system is to study behavior as the fish approach a large, fixed structure such as a hydroelectric dam. Such a typical tag deployment in front of a dam is shown in Figure 1. The depth of the water in front of the dam is assumed to be 50 m and the region of interest is the region in front of units 1, 2, and 3. For such an application it would be reasonable to locate the hydrophones on the opposite-diagonal corners of a 100 m × 100 m × 50 m deep "box". The lower, right-hand corner (location of hydrophone A) is the origin of the x, y, z coordinate system. The error expression in Appendix A has been evaluated for this

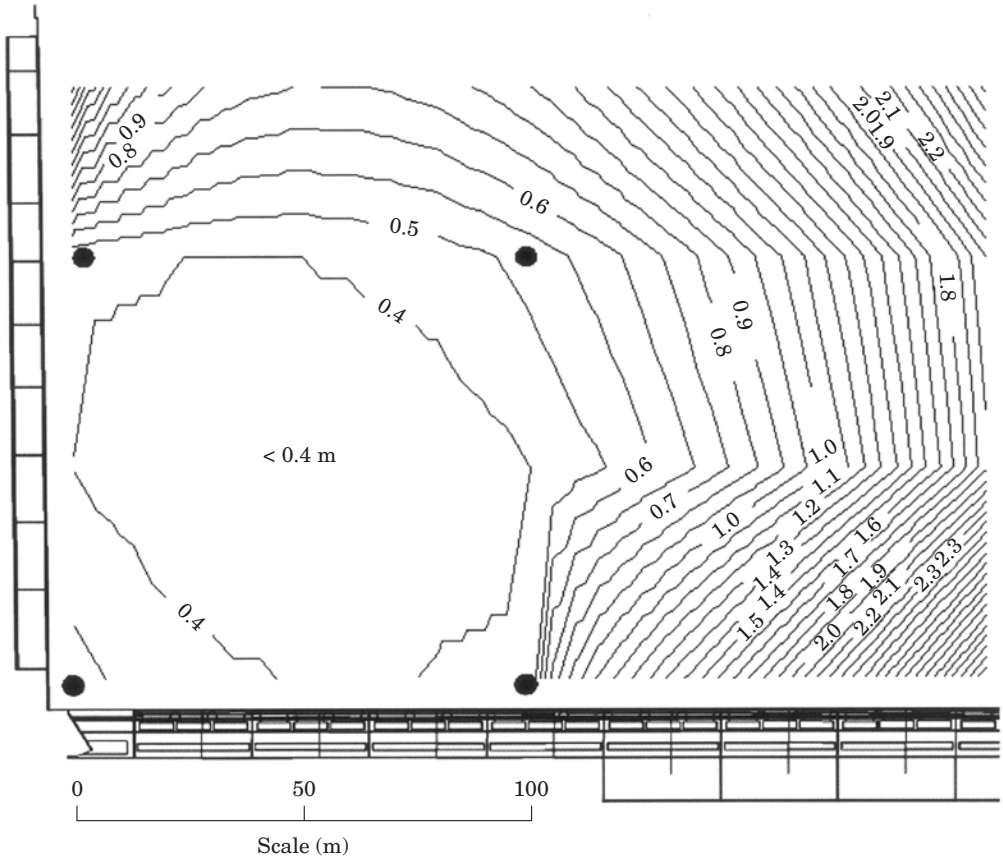

Figure 7. Plan view of the dam and hydrophone locations showing a contour plot of position errors for a depth of z=49 m.

hydrophone geometry as a function of the tag position along the dam (x), the distance out from the dam (y), and the depth (z). In general the signal-to-noise ratio at each hydrophone will be different and the analysis in Appendix A can accommodate these differences. To keep this example simple the standard deviation of the timing error for each of the four signals received at the hydrophones was assumed equal to 100 μs, which is 0.0001 s (this corresponds to a 1 ms long pulse and a signal-to-noise ratio of 20 dB). The r.m.s. value or standard deviation of the position error scales linearly with the timing-error standard deviation. Figure 2 shows the total r.m.s. position error for mid-water depth (z=26 m) as a function the location along the dam, x and three distances from the dam; y=50 m, 100 m, and 150 m. The error is minimized when the x position is in the center of the "hydrophone box" (x=y=50 m). The error increases at the edge of the box (y=100 m) and increases further when y is 50 m beyond the box (at y=150 m). It should also be noted that the error increases sharply when the position goes beyond the edge of the box in the x direction (i.e. when x is greater than 100 m). Figures 3 and 4 provide the same type of error results for a depth 49 m from the surface (i.e. z=1 m), and a depth that is 1 m from the surface (z=49 m). An alternative way to illustrate the error data is to use contour plots. Figures 5, 6, and 7 show for three depths, constant-error contours as a function of position in front of the dam. Both ways of presenting the results show that the error is small as long as the tag stays within the box defined by the hydrophones and gets larger as the tag moves outside of the confines of the box.

The effect of using an incorrect value of sound velocity is shown in Figure 8. The velocity error used in computing the curves in Figure 8 is 1 m s^{-1}. The total error, which is the square root of the sum of the squares of the three error components, scales linearly with velocity-error changes. The results in Figure 8 are for a depth in the center of the hydrophone box (z=25 m). The effects of temperature error on position accuracy can be determined by substituting Equation B4 into Equation A18. Figure 9 shows the r.m.s. position error for temperature errors of 0.05, 0.1, and 0.5°C along the edge of the "hydrophone box", (y =100 m). With care it is possible to determine the temperature with an

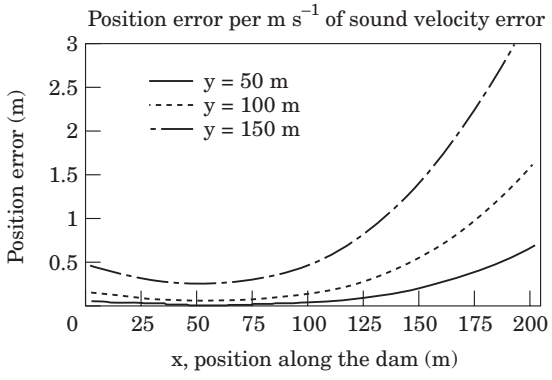

Figure 8. Tag location error for a velocity error of 1 m s^{-1} and a mid-water depth, z=25 m.

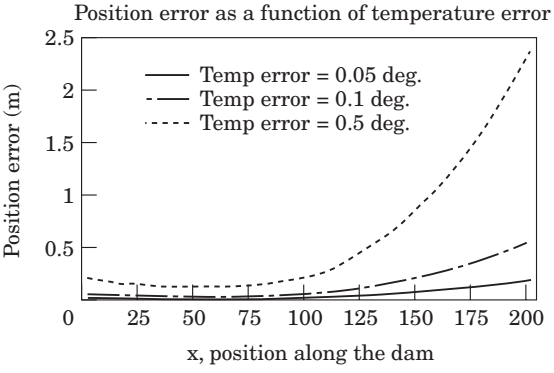

Figure 9. Tag location error as a function of temperature error in °C. Results shown for mid-water depth, z=25 m and edge on "hydrophone box", y=100 m.

accuracy of 0.1°C. It is clear that position error due to a 0.1°C temperature error is negligible within the "hydrophone box".

Appendix B also discusses the optimal selection of acoustic system parameters to achieve the minimum position errors. In particular it is shown that for the normal continuous wave (CW) pulse signal, the best performance is achieved by setting the pulse width equal to the minimum value that will insure sufficient signal-to-noise ratio to provide adequate tag detection at all locations in the region of interest. Although not considered here tag systems can use other types of signals called "wideband signals" that have much better performance for a given signal-to-noise ratio than present systems that use CW pulses.

Conclusions

The techniques developed in Appendix A and B provide a direct means of predicting the position accuracy of an acoustic tag that can be expected for a particular deployment of a tag system without the need for field measurements or Monte Carlo simulations. The techniques can be used during the design phase of a tag study to determine both the number of hydrophone required and the hydrophone placement in order to achieve a desired level of accuracy in the position estimates it provides. The calculations in the examples show that the errors are minimized when the tag is interior to the "box" defined by the receiving hydrophones. While the system will provide estimates outside the "hydrophone box" the errors can become quite large in some cases. The error analysis has also shown how the parameters of the acoustic system can be chosen to minimize the position errors. For example, the error due to additive noise for tags using CW pulse signals is minimized by selecting the shortest transmitted pulse length that provides the minimum signal energy required for pulse detection over the region of interest.

References

Clay, C. S., and Medwin, H. 1977. Acoustical oceanography, principles and applications. John Wiley, New York. 88 pp.

Hawkins, A. D., MacLennan, D. N., Urquhart, G. G., and Robb, C. 1974. Tracking cod, *Gadus morhua*, in a Scottish sea loch. Journal of Fish Biology, 6: 225–236.

Helstrom, C. W. 1960. Statistical theory of signal detection. Pergamon Press, New York.

Ireland, L. C., and Kanwisher, J. S. 1978. Underwater acoustic biotelemetry: procedures for obtaining information on the behavior and physiology of free-swimming aquatic animals in their natural environments. *In* The behavior of fish and other aquatic animals. Ed. by D. I. Mostofsky. Academic Press, New York.

Johnson, J. H. 1960. Sonic tracking of adult salmon at Bonneville Dam, 1957. Fishery Bulletin 176, United States Fish and Wildlife Service, Washington, DC.

Kell, L. T., Russell, I. C., and Challis, M. J. 1994. Proceedings of the IFM 25th annual study course. University of Lancaster, pp. 269–288.

Lacroix, G. L., and McCurdy, P. 1996. Migratory behavior of post-smolt Atlantic salmon during initial stages of seaward migration. Journal of Fish Biology, 49: 1086–1101.

Mitson, R. B. 1978. A review of biotelemetry techniques using acoustic tags. *In* Rhythmic activities of fishes, pp. 269–284. Ed. by J. E. Thorpe. Academic Press, New York.

Moore, A. 1995. The migratory behavior of wild Atlantic salmon (*Salmo salar*) smolts in the estuary of the River Conwy, North Wales. Canadian Journal of Fish and Aquatic Sciences, 529: 1923–1935.

Moore, A., Russell, I. C., and Potter, E. C. E. 1990. The effects of intraparitoneally implanted acoustic transmitters on the behavior and physiology of juvenile Atlantic salmon, *Salmo salar*. Journal of Fish Biology, 37: 713–721.

O'Dor, R. K., Andrade, Y., Webber, D. M., Sauer, W. H. H., Roberts, M. J., Smale, M. J., and Voegeli, F. M. 1998. Applications and performance of radio-acoustic positioning and telemetry (RAPT) systems. Hydrobiologia, 371/372: 1–8.

Parkinson, B. W., and Spilker, J. J. 1996. Global Positioning System: theory and applications, Volume I and II, American Institute of Aeronautics and Astronautics, Inc., Washington, DC.

Potter, E. C. E. 1988. Movements of Atlantic salmon, *Salmo salar L.*, in an estuary in south-west England. Journal of Fish Biology, 33: 153–159.

Potter, E. C. E., Solomon, D. J., and Buckley, A. A. 1992. Estuarine movements of adult Atlantic salmon, *Salmo salar* L., in Christchurch Harbour, southern England. *In* Wildlife telemetry – remote monitoring and tracking of animals, pp. 400–409. Ed. by I. G. Priede, and S. M. Swift. Ellis Horwood Ltd, Chichester.

Russell, I. C., Moore, A., Ives, S., Kell, L. T., Ives, M. J., and Stonehewer, R. O. 1998. The migratory behaviour of juvenile and adult salmonids in relation to an estuarine barrage. Hydrobiologia, 371/372: 321–333.

Smith, G. W., Urquhart, G. G., MacLennan, D. N., and Sarno, B. 1998. A comparison of theoretical estimates of the errors associated with ultrasonic tracking using a fixed hydrophone array and field measurements. Hydrobiologia, 371/372: 9–17.

Solomon, D. J., and Potter, E. C. E. 1988. First results with a new estuarine fish tracking system. Journal of Fish Biology, 33: 127–132.

Stasko, A. B., and Pincock, D. G. 1977. Review of underwater biotelemetry with emphasis on ultrasonic techniques. Journal of the Fisheries Research Board of Canada, 34: 1261–1285.

Steig, T. W. 2000. The use of acoustic tags to monitor the movement of juvenile salmonids approaching a dam on the Columbia River. Proceeding of the 15th International Symposium on Biotelemetry, Juneau, Alaska, 9–14 May 1999.

Steig, T. W., Adeniyi, R., Iverson, T. K., and Torkelson, T. C. 1999. Using acoustic tags for monitoring fine scale migration routes of juvenile salmonids in the forebay of Rocky Reach Dam in 1998. Report to Chelan County PUD No. 1, Wenatchee, Washington. Hydroacoustic Technology, Inc., Seattle, Washington.

Steig, T. W., Horchik, J. W., and Timko, M. A. 2001. Monitoring juvenile chinook and steelhead migration routes with acoustic tags in the forebay of the powerhouse and spillway of Rocky Reach Dam in 2000. Report to Chelan County PUD No. 1, Wenatchee, Washington. Hydroacoustic Technology, Inc., Seattle, Washington.

Steig, T. W., and Timko, M. A. 2000. Using acoustic tags for monitoring juvenile chinook and steelhead migration routes in the forebay of Rocky Reach Dam during the spring and summer of 1999. Report to Chelan County PUD No. 1, Wenatchee, Washington. Hydroacoustic Technology, Inc., Seattle, Washington.

Steig, T. W., and Timko, M. A. 2001. Feasibility study: assessing the viability of using acoustic tags for three-dimensional positioning at Lower Granite Dam. Report to US Geological Survey, Columbia River Field Station, Cook, Washington. Hydroacoustic Technology, Inc., Seattle, Washington.

Thorpe, J. E., Ross, L. G., Struthers, G., and Watts, W. 1981. Tracking Atlantic salmon smolts, Salmo salar, through Lock Voil, Scotland. Journal of Fish Biology, 19: 519–537.

Trefethen, P. S. 1956. Sonic equipment for tracking individual fish. Special Scientific Report – Fisheries Number 179, United States Fish and Wildlife Service, Washington, DC.

Voegeli, F. A., Lacroix, G. L., and Anderson, J. M. 1998. Development of miniature pingers for tracking Atlantic salmon smolts at sea. Hydrobiologia, 371/372: 35–46.

Appendix A

Derivation of the position error expressions

This appendix derives the expressions for the tag position error resulting from arrival-time measurement errors and from errors in the assumed value for the sound velocity. The error analyses do not depend on the details of the method used for extracting the tag position from the relative arrival times of the tag signal at the four hydrophones. The approach uses a differential analysis to find a linear approximation between the tag position and the timing error and sound-velocity error. The time required for the acoustic signal to travel a distance R_i between a tag with x,y,z coordinates a_1, a_2, a_3, and the ith hydrophone at position h_{i1}, h_{i2}, h_{i3} is given by:

$$t_i = \frac{1}{c} R_i = \frac{1}{c}\sqrt{(h_{i1}-a_1)^2+(h_{i2}-a_2)^2+(h_{i3}-a_3)^2}, \quad i = 1,2,3,4 \qquad \text{(A1)}$$

where c is the velocity of sound. An expression for the differential change in the arrival time, Δt_i, can be determined using partial derivatives:

$$\Delta t_i = \frac{1}{c}\left(\frac{\partial R_i}{\partial a_1}\Delta a_1 + \frac{\partial R_i}{\partial a_2}\Delta a_2 + \frac{\partial R_i}{\partial a_3}\Delta a_3\right) + \Delta t_m \qquad \text{(A2)}$$

where Δa_1, Δa_2, Δa_3 are the differential changes in the x,y,z location of the tag, and $\Delta t_m$is the measurement error due to a difference in the actual and assumed crystal frequency of the receiver's analog to digital converter. The differential arrival-time equations for the four arrival times can be written in matrix form as

$$\Delta t = D\Delta a \qquad \text{(A3)}$$

where:

$$\Delta t = \begin{pmatrix} \Delta t_1 \\ \Delta t_2 \\ \Delta t_3 \\ \Delta t_4 \end{pmatrix}, \quad D = \begin{pmatrix} d_{11} & d_{12} & d_{13} & 1 \\ d_{21} & d_{22} & d_{23} & 1 \\ d_{31} & d_{32} & d_{33} & 1 \\ d_{41} & d_{42} & d_{43} & 1 \end{pmatrix}, \quad \Delta a = \begin{pmatrix} \Delta a_1 \\ \Delta a_2 \\ \Delta a_3 \\ \Delta t_m \end{pmatrix} \qquad \text{(A4)}$$

and:

$$d_{ij} = \frac{1}{c}\frac{\partial R_i}{\partial a_j} = \frac{h_{ij}-a_j}{cR_i}, \quad i = 1,2,3,4 \text{ and } j = 1,2,3 \qquad \text{(A5)}$$

Using simple matrix algebra it follows that the location error vector, Δa, can be related to the variability in the arrival-times variability vector, Δt, by:

$$\Delta a = D^{-1}\Delta t \qquad \text{(A6)}$$

The mean squared arrival-time error is determined by evaluating the position error covariance matrix, P_e:

$$P_e = E[\Delta a \Delta a^T] = E[D^{-1}\Delta t (D^{-1}\Delta t)^T] \qquad \text{(A7)}$$

where E[ ] is the expectation operator. Using the properties of the transpose of matrices and using the fact that the matrix D is not random results in:

$$P_e = E[\Delta a \Delta a^T] = D^{-1}\, E[\Delta t \Delta t^T]\, (D^{-1})^T \quad \text{(A8)}$$

It is reasonable to assume that the variability in the travel times at the individual hydrophones are statistically independent and zero mean. It therefore follows that:

$$E[\Delta t(\Delta t)^T] = \begin{pmatrix} \sigma_{t1}^2 & 0 & 0 & 0 \\ 0 & \sigma_{t2}^2 & 0 & 0 \\ 0 & 0 & \sigma_{t3}^2 & \\ 0 & 0 & 0 & \sigma_{t4}^2 \end{pmatrix} \quad \text{(A9)}$$

where σ_{ti}^2 is variance in the arrival-time measurement at the ith hydrophone. When the variances for each of the arrival times are equal:

$$E[\Delta t(\Delta t)^T] = \sigma^2\, I \quad \text{(A10)}$$

where I is a 4 by 4 identity matrix and:

$$P_e = E[\Delta a \Delta a^T] = \sigma^2\, D^{-1}\, (D^{-1})^T \quad \text{(A11)}$$

The first three diagonal elements of the position error covariance matrix P_e are the variances in the x, y, and z location estimates:

$$\sigma_x^2 = P_{e11},\ \sigma_y^2 = P_{e22},\ \sigma_z^2 = P_{e33} \quad \text{(A12)}$$

The total variance of the position estimate, σ_p, is:

$$\sigma_p = \sqrt{\sigma_x^2 + \sigma_y^2 + \sigma_z^2} \quad \text{(A13)}$$

There are three factors that can result in timing errors: (1) additive noise that affects the measured arrival time the signal is received at the hydrophone, (2) "quantization" noise that occurs when the measured analog arrival time is converted into a discrete digital number, and (3) multipath effects. The effects of additive noise and quantization will be quantified below. Multipath effects are much more difficult to deal with. When a direct-path signal and a reflected-path signal interact, the amplitude, phase and shape of the combined signal is affected. Consequently the measured arrival time can differ from that of the direct signal alone. The actual timing cannot be accurately predicted since they depend on so many variables such as: the number of reflected signals, the relative amplitude and phases of direct and reflected signals, relative time delays of the direct and reflected signal, etc. However the above analysis can be used if empirical data can be used to quantify the effect of "multipath" in terms of the RMS error in the arrival time at each hydrophone.

The relationship between sound-velocity errors and tag-position errors is determined by, first rewriting Equation (A1) as:

$$ct_i = R_i = \sqrt{(h_{i1} - a_1)^2 + (h_{i2} - a_2)^2 + (h_{i3} - a_3)^2}, \quad i = 1,2,3,4 \quad \text{(A14)}$$

The differential change in the velocity of sound is related to the position errors using partial derivatives.

$$\Delta R_i = \Delta c t_i = \left(\frac{\partial R_i}{\partial a_1} \Delta a_1 + \frac{\partial R_1}{\partial a_2} \Delta a_2 + \frac{\partial R_i}{\partial a_3} \Delta a_3 \right) + \Delta R_m, \quad i = 1,2,3,4 \quad \text{(A15)}$$

where ΔR_m is the error in the range calculation due to differences between the measured and assumed sampling frequency of the analog-to-digital converter. Writing Equation (A15) in matrix form gives:

$$\Delta c \begin{pmatrix} t_1 \\ t_2 \\ t_3 \\ t_4 \end{pmatrix} = M \begin{pmatrix} \Delta a_1 \\ \Delta a_2 \\ \Delta a_3 \\ \Delta R_m \end{pmatrix} \quad \text{(A16)}$$

where:

$$M = \begin{pmatrix} m_{11} & m_{12} & m_{13} & 1 \\ m_{21} & m_{22} & m_{23} & 1 \\ m_{31} & m_{32} & m_{33} & 1 \\ m_{41} & m_{42} & m_{43} & 1 \end{pmatrix} \text{ and } m_{ij} = \frac{\partial R_i}{\partial a_i} = \frac{h_{ij} - a_j}{R_i} \quad \text{(A17)}$$

Using matrix algebra, it follows that:

$$\begin{pmatrix} \Delta a_1 \\ \Delta a_2 \\ \Delta a_3 \\ \Delta R_m \end{pmatrix} = M^{-1} \begin{pmatrix} t_1 \\ t_2 \\ t_3 \\ t_4 \end{pmatrix} \Delta c \quad \text{(A18)}$$

Appendix B

Arrival-time errors, velocity errors, and optimization of performance

There are various acoustic effects that can cause errors in the measured, relative arrival times of the signals at the reference hydrophones. Two of these factors will be considered in this appendix. It will also discuss the primary factor that can cause an error in the assumed sound velocity.

Arrival time errors

Acoustic noise will cause measurement errors in the arrival-time measurement. Fortunately the effect of noise on arrival-time measurements has been previously studied in the analysis of radar, sonar and communications systems. These previous analyses have shown that for matched filter receiver designs, the standard deviation in the arrival time is given by:

$$\sigma_{rms} = \frac{1}{\sqrt{SNR_o BW}} \tag{B1}$$

where SNR_o is the ratio of the signal-power-to-noise-power out of the matched filter and BW is the baseband, signal bandwidth. In the case of the standard CW pulse signal, the baseband bandwidth, BW, is the reciprocal of the pulse length T. For example, 1 ms long CW pulse signal has a baseband bandwidth of $1/0.001 = 1000$ Hz. If the received signal level is ten times greater than the noise standard deviation out of the matched filter ($SNR_0 = 100$ or 20 dB) then using Equation (B1), the standard deviation of the arrival-time measurement is 0.1 ms.

Another potential source of arrival-time errors is the quantization error due to the fact that the digital processing system breaks the time up into discrete increments.

The difference between the true time and the discrete representation of time is called the quantization noise. It can be shown that the standard deviation value of the quantization error is:

$$q_{rms} = \frac{\Delta}{2\sqrt{3}} = \frac{1}{2\sqrt{3} f_s} \tag{B2}$$

where Δ is the sampling interval and f_s is the sampling frequency. Hence the standard deviation for a system using a 12 kHz sampling rate is $2.4 \times 10^{-5} = 0.0024$ ms. In most cases the size of the quantization noise is small compared to the arrival-time errors due to the effect of additive noise.

Velocity error

The velocity of sound in fresh water can be accurately predicted if the water temperature is known. In particular, the velocity of sound, c, can be written as:

$$c = 14449.2 + 4.6T - 0.055T^2 + 0.00029T^3 + (1.34 - 0.010T)(S - 35) + 1.58 \times 10^6 P_a \tag{B3}$$

where c = velocity of sound (m s^{-1})
T = temperature in °C
S = salinity
P_a = static water pressure (N/m^2).

The variation in sound velocity with temperature changes is determined by differentiating Equation (B3) with respect to T:

$$\Delta c = [4.6 - 0.11T + 0.00087T^2 - 0.010(S - 35)]\Delta T \tag{B4}$$

For fresh water and a nominal temperature of 10°C, the speed of sound changes about 3.9 m s^{-1} for each °C. With care it is possible to determine the temperature to within a fraction of a °C, and, consequently, the sound-velocity error can be made quite small. This expression for the sound-velocity error can be used in Equation (A18) to obtain an expression for position error as a function of temperature error.

Performance optimization

From the discussion in this appendix it is clear that acoustic tag systems should include provisions for accurately measuring the water temperature and thereby minimize the error in the velocity of sound used in the equations for the calculation of position. Similarly, the sampling rate should be sufficiently high to assure that the effect of quantization noise is negligible. Selection of system parameters to minimize the adverse effect of additive noise is not as obvious. From Equation (B1), it is clear that the arrival-time error is inversely proportional to both the signal-to-noise ratio and the bandwidth. Unfortunately for normal CW pulse tag systems it is not possible to increase independently both these variables. As the bandwidth of the signal is increased the level of the noise passing through the receiver filter also increases and the signal-to-noise ratio decreases. Re-writing Equation (B1) to include these relationships yield the following expression for the timing-error variability:

$$\sigma_{rms} = \frac{k}{\sqrt{BW}} \tag{B5}$$

where k is a constant. The bandwidth for CW pulse signals is equal to the reciprocal of the pulse length, T, and therefore:

$$\sigma_{rms} = k\sqrt{T} \tag{B6}$$

The conclusion that can be drawn from Equation (B6) is that the performance is improved as the pulse width is made shorter. However as the pulse width is decreased the energy in the signal received at the hydrophones is decreased. If the pulse width is too short the signal level will be too small for the received pulse to be detected. Therefore the pulse width should be great enough to ensure that there is sufficient signal-to-noise for pulse detection (at least 10 dB) at all ranges of interest.

From the discussion above it is clear that there are conflicting requirements that must be considered in selecting the pulse width. On one hand the pulse width should be short to minimize the timing error variability but on the other, the pulse width must be long enough to provide sufficient signal energy for pulse detection. This dilemma could be avoided if tag systems used wideband signals rather than CW pulses. Using wideband signals it is possible to achieve independently both the high bandwidth required for minimum timing errors and the high signal energy required for signal detection.